SHEAR COAXIAL INJECTOR INSTABILITY MECHANISMS

C. Puissant[†], T. Kaltz[+], M. Glogowski[+] and M. Micci[*]
Department of Aerospace Engineering & Propulsion Engineering Research Center
The Pennsylvania State University
University Park, PA 16802

OVERVIEW

There is no definitive knowledge of which of several concurrent processes ultimately results in unstable combustion within liquid rocket chambers employing shear coaxial injectors. Possible explanations are a detrimental change in the atomization characteristics due to a decrease in the gas-to-liquid velocity ratio, a change in the gas side injector pressure drop allowing acoustic coupling to the propellant feed system or the disappearance of a stabilizing recirculation region at the base of the LOX post. The aim of this research effort is to investigate these proposed mechanisms under conditions comparable to actual engine operation. Spray characterization was accomplished with flash photography and planar laser imaging to examine the overall spray morphology and liquid jet breakup processes and with a PDPA to quantify the spatial distribution of droplet size and mean axial velocity. A simplified stability model based on the Rayleigh criterion was constructed for the flow dynamics occurring within the chamber and injector to evaluate the potential coupling between the chamber and injector acoustic modes and was supported by high frequency measurements of chamber and injector pressure oscillations. To examine recirculation within the LOX post recess, velocity measurements were performed in the recess region by means of LDV. Present experiments were performed under noncombusting conditions using LOX/GH$_2$ simulants at pressures up to 4 MPa.

DISCUSSION

The laboratory injector used in these experiments was modeled after the injector element of the SSME fuel preburner and included two LOX post tip shapes, tapered and nontapered. Liquid nitrogen and gaseous nitrogen served as the principle simulants to liquid oxygen and gaseous hydrogen, respectively. Injector characterization was performed in an optically accessible pressure chamber. To evaluate the feasibility of laser Doppler velocimetry within the recess region of the injector, water and air were used but at reduced mass flow rates.

Spray Visualization Experiments

The effect of chamber pressure and gas mass flow rate on spray morphology was examined at liquid-to-gas mixture ratios of 0.78 and 1.57 with a liquid nitrogen mass flow rate of

---

† Adjunct Research Assistant, + Graduate Research Assistant, * Associate Professor

0.050 kg/s. Fig. 1 depicts the photographic results from three representative experiments using the planar laser imaging technique. As can be seen from Figs. 1a and 1b, increasing chamber pressure effects a contraction of the large scale liquid structures (liquid core and detached ligaments) and droplet flow regions observed downstream of the dense liquid structures. This trend would suggest an enhancement in the rate of liquid vaporization with increasing chamber pressure through a combined reduction in the latent heat of vaporization and liquid surface tension. In Fig. 1c the result of decreasing gas mass flow rate, or increasing mixture ratio, was a larger, more dispersed spray suggesting a strong influence of the gas mass flow rate on the atomization and vaporization of liquid nitrogen. In terms of droplet sampling with the PDPA, these reduced gas flow conditions are advantageous in that the dilute spray region is spread over a larger volume.

Additional tests were performed with the tapered LOX post using a stroboscope to visualize the spray. In general, the stroboscopic image provides more detail on the structure of the liquid core and detached ligaments than the laser sheet images but less information on the droplet flow region. Figs. 2a and 2b depict the structure of the jet issuing from the injector at sub- and supercritical pressures. Contradictory to the observed contraction of the spray with increasing pressure, the liquid core breakup length has increased for a supercritical chamber pressure ($P_c > 3.4$ MPa). This behavior may be attributed to the drop in relative velocity between the gas and liquid at very high chamber pressures, which may surpass any enhancements to liquid breakup due to increased gas density, or to the increase in droplet evaporation times observed in the supercritical region. Stroboscope tests with the nontapered LOX post under similar operating conditions revealed the same behavior for sub- and supercritical pressures but indicated little difference in spray morphology between the two LOX post designs.

Droplet Size and Velocity Measurements

Droplet size and velocity measurements were obtained at three mixture ratios, 2.2, 1.6 and 1.1, for a LN_2 mass flow rate of 0.072 kg/s. The effect of chamber pressure on droplet size and mean axial velocity was found to be negligible as is seen from tests B1 and B2 of Table 1. Interestingly, the number of droplets sampled during a fixed interval of the tests decreased dramatically with increasing chamber pressure due to the contraction of the spray at higher pressures and/or a change in optical alignment as a result of increased gas density. The results for tests B2 to B4 show an expected decrease in droplet mean axial velocity when moving radially outward in the spray and an increase in velocity when moving closer to the injector. Negligible change in droplet size as represented by D_{10} was observed for all three tests. The effect of decreasing mixture ratio is seen from tests B4, B5 and B6. Test B5 and B6, performed at the same location in the spray, show an increase in drop mean velocity with decreasing
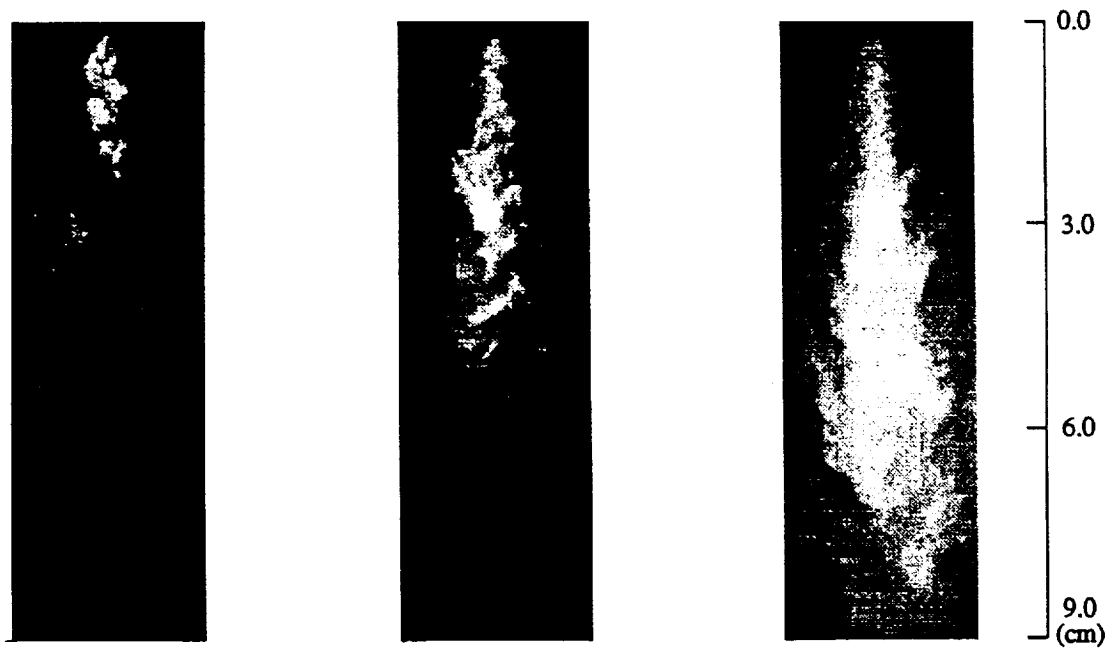
(a) 2.93 MPa (MR: 0.78)   (b) 2.32 MPa (MR: 0.78)   (c) 2.34 MPa (MR: 1.57)

Fig. 1 Effect of chamber pressure and mixture ratio on LN_2/GN_2 spray.
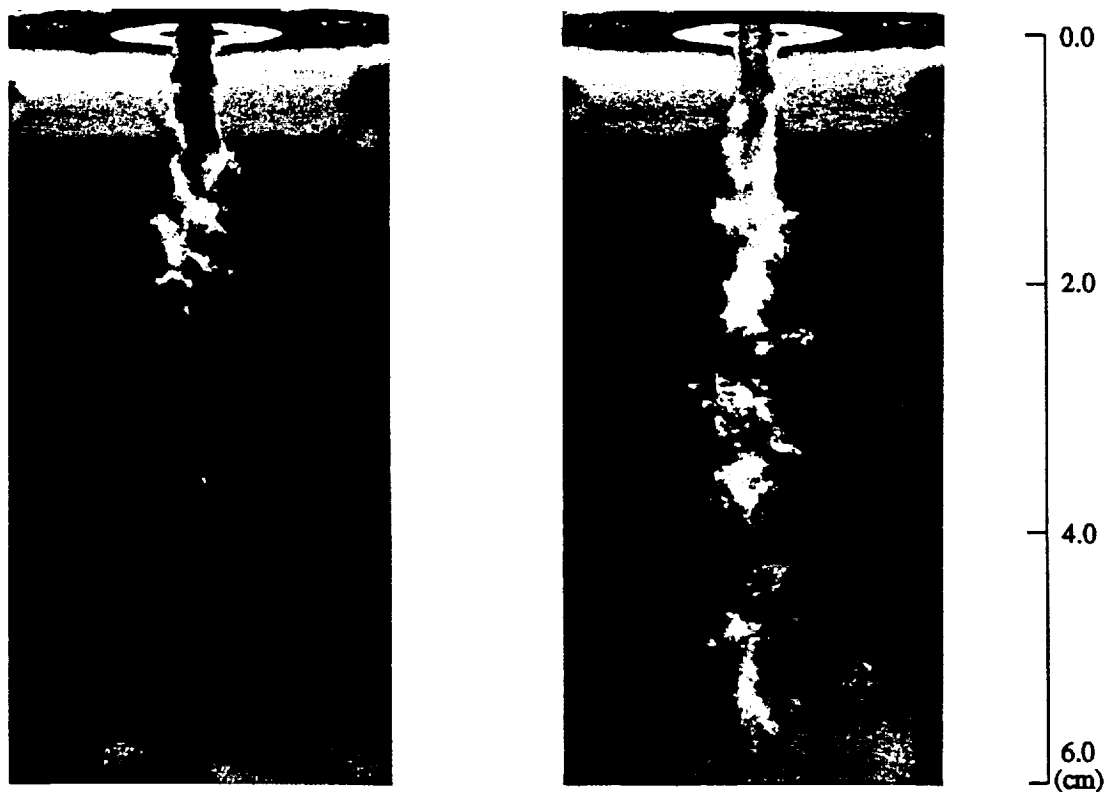
(a) 2.94 MPa   (b) 3.97 MPa

Fig. 2 Stroboscope results for tapered LOX post at sub- and supercritical pressures (MR: 0.81).

Table 1. Operating Conditions and Droplet Size and Velocity Data for PDPA Tests.

Test No.	P_c (MPa)	$\dot{m}_l/\dot{m}_g$	U_g/U_l	Pos. (cm)		U_{drop} (m/s)	Droplet Size (μm)		No. Droplets
				Z	R		D_{10}	D_{32}	
B1	2.63	2.24	3.87	12	0	15.9	10.1	96.7	512
B2	2.40	2.19	4.20	12	0	14.4	11.2	97.3	2514
B3	2.37	2.15	4.30	12	0.5	9.3	12.9	91.6	375
B4	2.41	2.20	4.23	10	0	14.8	14.1	105.5	562
B5	2.45	1.60	5.74	10	0	20.8	7.5	110.3	151
B6	2.37	1.14	7.53	6	0	37.1	8.4	118.3	121

mixture ratio due to the higher gas exit velocity. The effect of mixture ratio on spray drop size is presented as the superposition of the three drop size distributions in Fig. 3. With increasing gas mass flow rate, or decreasing mixture ratio, the majority of droplets shift to smaller size ranges. The large difference between the arithmetic mean diameter and Sauter mean diameter listed in Table 1 arose from the bimodal size seen in Fig. 3. The small number of large droplets at the upper end of the size range, observed during all of the tests, may be due to remnants of the liquid core, coalesced small droplets or instrument misinterpretation of the collected signal.
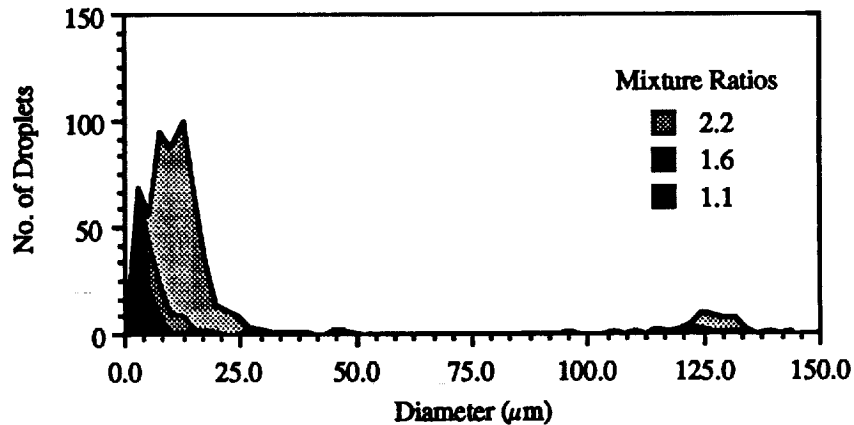
Fig. 3 Droplet size distribution for three oxidizer to fuel mixture ratios (P_c = 2.4 MPa).

Analytical Modeling

The injector response was calculated from the analytical model using only the processes of gas flow through the injector and the nozzle. The response was determined as a function of frequency and gaseous fuel temperature for the experimental conditions experienced during the cold flow LN$_2$/GN$_2$ experiments. During these experiments, high frequency pressure oscillations were measured in the chamber and the injector fuel plenum. Fig. 4 shows the injector response as a function of fuel temperature for several frequencies. It can be seen that at high frequencies the response is near zero, at intermediate frequencies the response is negative

and almost constant and at low frequencies the response becomes strongly positive as the fuel temperature decreases. The recorded high frequency pressure oscillations were spectrally analyzed to determine the frequencies and magnitudes of any acoustic oscillations within either the chamber or the injector fuel plenum. Oscillations at the same frequency in both the chamber and the plenum were found at two frequencies, 2000 and 5800 Hz. The calculated injector response at those two frequencies correlated well with the measured ratios of the pressure oscillation amplitude in the chamber to the amplitude in the plenum.

Recirculation Region

To permit LDV access to the recess region the injector was modified by inserting a Pyrex tube concentrically around the nontapered LOX post, such that the fuel annulus became a transparent boundary, 1.02 mm thick. Water was used as the LOX simulant and air for the gaseous fuel simulant. Measurements of mean axial velocity were taken inside the injector recess region as well as downstream of the injector. Downstream of the injector face only positive velocities were measured. Within the recess region several axial and radial scans revealed evidence of recirculation. Fig. 5 shows the droplet velocity near the center of the LOX post tip landwidth as a function of axial distance from the LOX post tip. The air flow rate was 1.8 g/s and the water flow rates were 1.9 and 4.5 g/s. It can be seen that the velocity drops to a negative value approximately 0.5 mm downstream of the LOX post base before becoming positive. Larger negative values of the velocity were observed for lower liquid flow rates. Thus, it appears that gas recirculation does exist in the recess region of a shear coaxial injector element and that the strength of the recirculation is a function of the operating conditions.
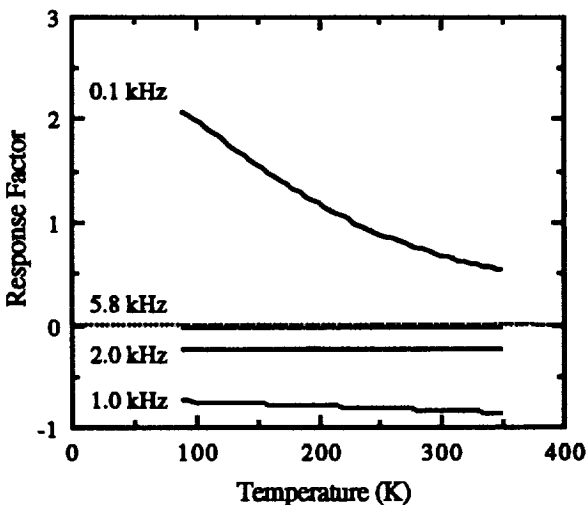
Fig. 4 Injector response as a function of gaseous fuel temperature for several frequencies.
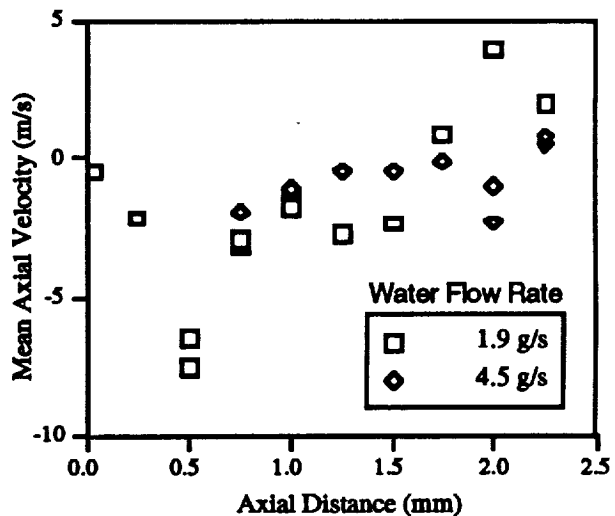
Fig. 5 Droplet mean axial velocity as a function of axial distance within the injector recess region.

210